

C. TEICHERT<sup>1,✉</sup>  
G. HLAWACEK<sup>1</sup>  
A.YU. ANDREEV<sup>1,2</sup>  
H. SITTE<sup>2</sup>  
P. FRANK<sup>3</sup>  
A. WINKLER<sup>3</sup>  
N.S. SARICIFTCI<sup>4</sup>

## Spontaneous rearrangement of para-sexiphenyl crystallites into nano-fibers

<sup>1</sup> Institute of Physics, University of Leoben, Franz Josef Straße 18, 8700 Leoben, Austria

<sup>2</sup> Institute for Semiconductor and Solid State Physics, University Linz, 4040 Linz, Austria

<sup>3</sup> Institute of Solid State Physics, Graz University of Technology, Petersgasse 16, 8010 Graz, Austria

<sup>4</sup> Linz Institute of Organic Solar Cells, University Linz, 4040 Linz, Austria

Received: 10 October 2005/Accepted: 26 October 2005

Published online: 1 December 2005 • © Springer-Verlag 2005

**ABSTRACT** In the growth of para-sexiphenyl films on mica(001), an interesting phenomenon was observed where small individual crystallites spontaneously arrange into parallel running high-aspect ratio chains with a length in the micrometer range. A statistical analysis of the chain dimensions reveals a very narrow length distribution and the existence of a threshold length. The observation of denuded zones around the chains and the interior chain structure suggest a rearrangement of the crystallites as entities. It is proposed that this spontaneous rearrangement is driven by the formation of a one-dimensional defect array which evolves within the monomolecular para-sexiphenyl wetting layer when a critical crystallite density is reached.

**PACS** 81.07.Nb; 81.10.Bk; 81.16.Dn; 68.37.Ps

### 1 Introduction

In the field of thin film deposition, researchers' efforts were focused for a long time on the formation of smooth epitaxial films. With the emergence of nano-science and technology, the spontaneous evolution of three-dimensional nanostructures during epitaxial growth is now of superior importance. A prominent example is the strain-driven self-organization of nanostructures in semiconductor heteroepitaxy. This phenomenon, first found for conventional, inorganic semiconductor systems [1, 2] is also observed for organic ones [3–6].

In this work, atomic-force microscopy was used to follow in detail the morphology evolution of para-sexiphenyl films grown on mica(001). The previously found, very long high aspect ratio needles (fibers) [7–9], could be resolved into chains of three-dimensional (3D) islands (crystallites). These straight chains form spontaneously as soon as a critical density of isolated crystallites

on the surface is present. As shown previously the chains run parallel to each other and their orientation is determined by the surface geometry of the substrate and is not influenced by surface steps [6, 7, 10]. Further growth is characterized by a coexistence of these self-organized crystallite chains with micrometer length and individual isolated crystallites (typical  $100 \times 50 \times 20$  nm in size). Analysis of the chain length for different surface coverages reveals very narrow length distributions and the existence of a minimum chain length. The observation of denuded zones around the chains and the interior chain structure resolved by high-resolution atomic-force microscopy suggests that this self-alignment process is based on the rearrangement of the crystallites as entities.

### 2 Experimental techniques

The para-sexiphenyl (p-6P) [11] was cleaned by a threefold sublimation process in dynamic vacuum. As

the substrate, freshly cleaved mica(001) was used. After insertion into the growth chamber the mica substrates were preheated at 360 K for 30 minutes to remove surface contaminations such as water. The growth chamber of the hot wall epitaxy (HWE) system used [7, 12], contains a separate preheating/annealing oven and two HWE reactors for the deposition. Each reactor has three ovens that can be heated independently. This setup allows the selecting of individual temperatures for the wall and the source zones. At the bottom of the source zone a quartz glass tube holds the p-6P. The substrate was placed close to the tube end and could be heated separately. This semiclosed growth system guarantees a nearly uniform and isotropic flux of the molecules onto the substrate surface and is proven as very appropriate for Van der Waals epitaxy of large organic molecules [7, 12]. The vacuum during growth was  $6 \times 10^{-6}$  mbar. Source and substrate temperature were 510 K and 360 K, respectively. The wall temperature was in the range of 510–530 K.

Thermal desorption spectroscopy (TDS) was performed in an UHV chamber (base pressure  $10^{-10}$  mbar). The amount of deposited p-6P material was measured quantitatively with a quartz microbalance. For TDS the sample was attached to a resistively heated steel substrate which was heated at a rate of 1 K/s. The desorbing species were detected with a quadrupole mass spectrometer [13].

The films were investigated ex-situ by atomic-force microscopy (AFM). A Digital Instruments MultiMode IIIa scanning probe microscope with an AS-130(J) scanner was used. All measurements were done under ambient con-

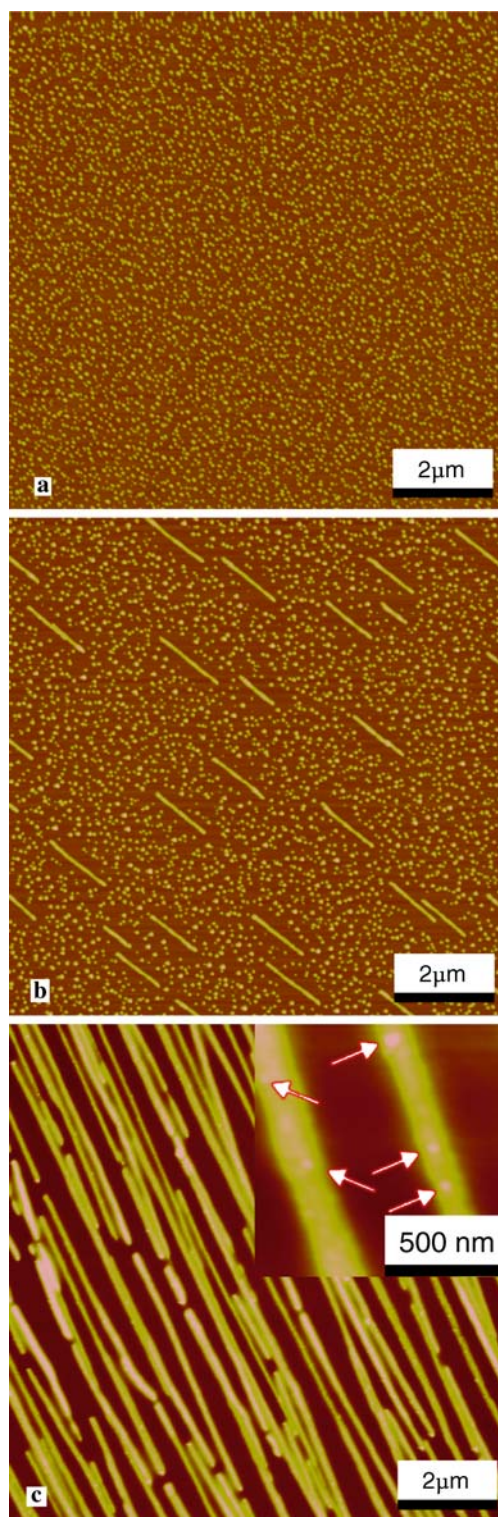
✉ Fax: +43 3842 402-4602, E-mail: teichert@unileoben.ac.at

ditions using tapping mode to eliminate the risk of surface damage due to lateral forces between tip and surface. Most of the presented images have been obtained with Pt-coated Si-tips. Some of the high resolution images were recorded using high density carbon (HDC) tips. These tips consist of a carbon whisker attached to a conventional Si-tip. These probes have a tip radius of less than 5 nm and an opening angle of less than  $10^\circ$ . The resulting high aspect ratio allows precise imaging of crystallites with nearly vertical side walls. In order to access statistical information on the growth process, at least 100 objects per growth stage were analyzed.

### 3 Results and discussion

Figure 1 shows representative images of the three different stages of p-6P growth on mica(001). The first stage is shown in Fig. 1a and is characterized by the formation of randomly distributed crystallites with uniform size of about  $100 \times 50 \times 10$  nm (length  $\times$  width  $\times$  height). Obviously, the crystallites repel each other at this stage since we never found a coalescence of crystallites. The surface morphology changes drastically as soon as a critical density of islands is reached between 30 and 35 seconds of growth: a rearrangement of crystallites occurs resulting in self-organized parallel chains coexisting with isolated crystallites (intermediate growth stage as shown in Fig. 1b). With increasing time these chains become progressively longer and closer to each other, whereas the isolated crystallites disappear. Figure 1c shows the corresponding advanced growth stage after 9 minutes. The surface structure here is made up only of parallel chains with a very high aspect ratio in length.

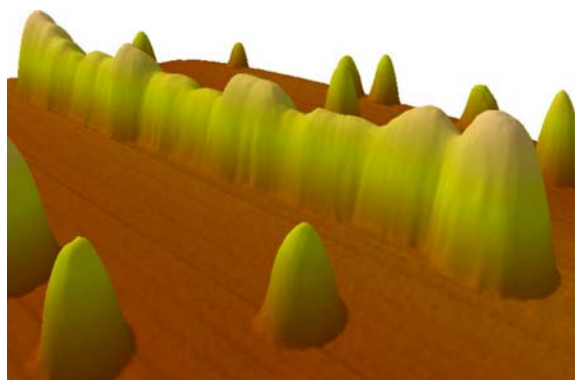
Figure 2 shows a detailed AFM scan of a single chain in an intermediate stage. This chain is 850 nm long and has a height and width of 15 nm and 75 nm, respectively. The size of the features within the chain and that of the crystallites which surround the chain are equal. It seems that the displayed chain is made up from approximately 14 crystallites. It is important to mention here that much longer chains also show the same internal structure as such a shorter one shown in Fig. 2.



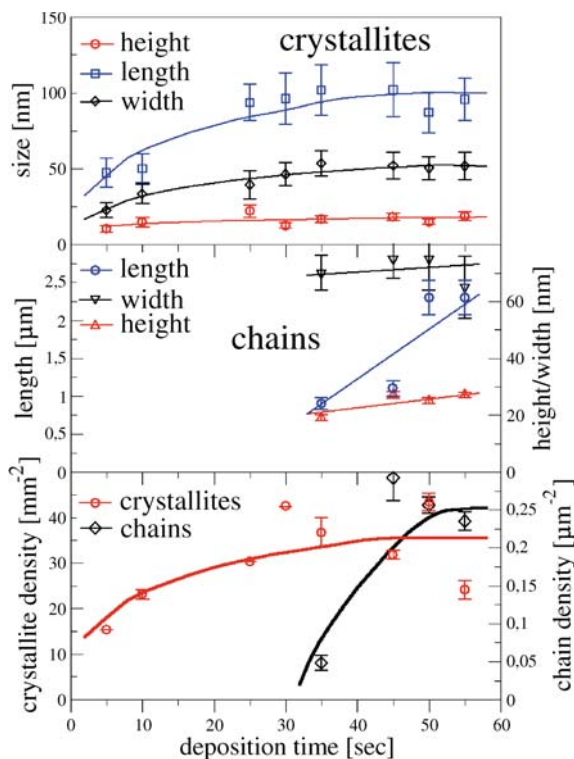
**FIGURE 1** Different growth stages of p-6P films on mica. Pure island growth after 30 sec (a); islands (crystallites) and chains after 45 sec (b); long term growth morphology after 9 min, consisting only of chains (c). The inset in (c) shows a higher resolution scan, revealing that in this stage small crystallites are formed on top of the chains. z-scale for all pictures is 50 nm

Figure 3 presents the crystallite size and density evolution over the first 60 seconds of p-6P deposition. One can see that the crystallites reach their final height of 18 nm after 10 seconds and their final width and length, of 50 nm and 100 nm, after approximately 30 to 35 seconds (first stage). Simultaneously

the crystallite density increases continuously and reaches a saturation value of  $35 \mu\text{m}^{-2}$ . The first chains appear after approximately 35 seconds of the p-6P deposition marking the beginning of the intermediate growth stage, in which individual crystallites and chains coexist. From this time, size and the density of



**FIGURE 2** Detailed 3D-image of a single 850 nm long chain after 35 seconds of p-6P deposition (intermediate stage) revealing the interior structure of the chain.  $1 \times 1 \mu\text{m}$  scan,  $z$ -scale is 30 nm



**FIGURE 3** Evolution of length, width and height as well as density of crystallites and chains. Continuous lines are just guides to the eye

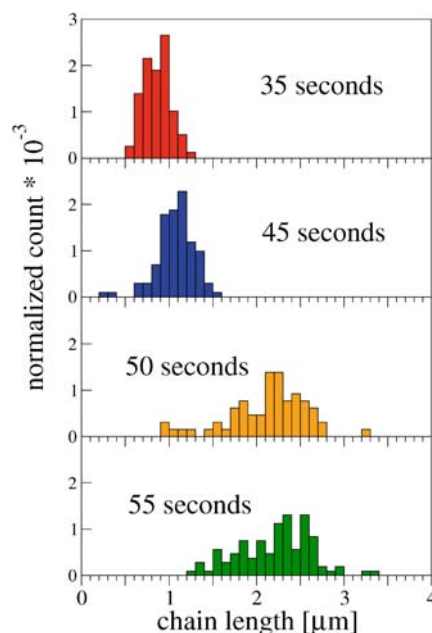


**FIGURE 4** Evolution of chain length distribution as a function of deposition time from 35 to 55 seconds

the crystallites do not increase anymore and saturate at the values given above. In contrast, the chain length strongly increases from 800 nm to 2000 nm between 35 and 55 sec of deposition. However, their width and height increase much slower.

Figure 4 shows the evolution of the chain length distributions in the intermediate stage. One can see that at the beginning (35 sec) the chains exhibit a very narrow length distribution with an average length of 800 nm (see also Figs. 1–3). The minimum and maximum chain lengths here are around 500 nm and 1300 nm, respectively. If more material is deposited, the average chain length increases and the chain length distribution slightly broadens. Most important, however, is the exist-

tence of a threshold length, below which the chains seem to be energetically unstable. This threshold length depends on surface coverage, namely it increases from 500 nm (about 10 crystallites) after 35 seconds of deposition to 1200 nm (about 24 crystallites) after 55 seconds (see Fig. 4).

As can clearly be seen from Fig. 5, in the intermediate stage the chains are surrounded by a denuded zone that is free of crystallites. This denuded zone is found at all four sides of the chains. In Fig. 5 two rectangles of the same size are drawn. The number of crystallites in the lower rectangle is approximately equal to the number of crystallites needed to form the chain in the upper rectangle. From this observation and from the interior chain structure we con-

clude that the chains are spontaneously formed by rearrangement of the individual crystallites as entities. This idea is also supported by recent selected area electron diffraction and TEM measurements, which revealed the existence of three differently oriented p-6P domains within the chains [14].

Before we discuss the growth morphology evolution in detail we want to add another experimental detail that is related to the question whether the crystallites grow directly on the mica substrate or on a continuous p-6P wetting layer. Surface roughness measurements by AFM revealed a significant increase of the root mean square (rms) roughness if we compare the mica substrate (0.1 nm) with areas of the p-6P covered sample in between the crystallites or chains (0.5 nm) [7]. This observation might be an indirect hint towards the existence of a p-6P wetting layer.

The direct proof for the existence of such a wetting layer arises from thermal desorption spectra presented in Fig. 6. For small coverages one observes a desorption peak at around 550 K, which saturates at a mean coverage of 0.2–0.3 nm. Considering the Van der Waals dimensions of p-6P ( $0.35 \times 0.67 \times 2.85 \text{ nm}^3$ ) this is a clear indication that a rather strongly bonded wetting layer of flat lying molecules exists. For higher coverages, a second peak

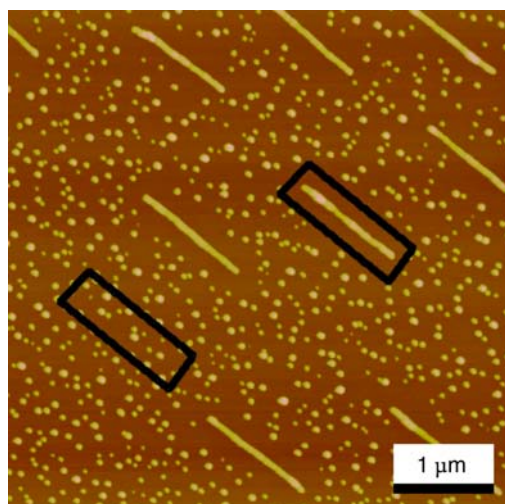


**FIGURE 5** AFM image revealing denuded zones around chains. The amount of material in the lower rectangle is approximately equal to the amount of material needed to build the chain in the upper rectangle. z-scale is 50 nm

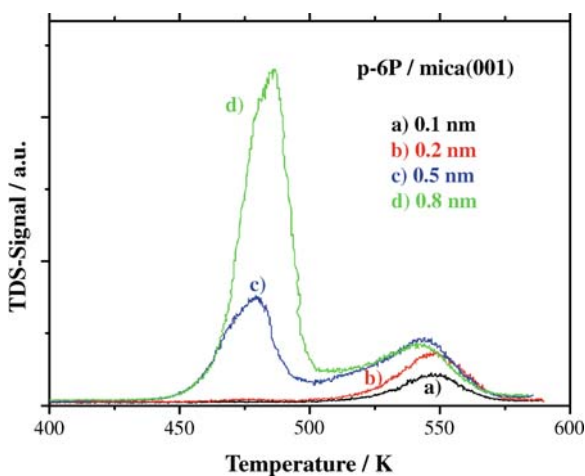


**FIGURE 6** Thermal desorption spectra for p-6P on mica(001). Adsorption temperature 360 K, heating rate 1 K/s. The mean thickness of the individual films as measured with the quartz microbalance is indicated

arises at around 480 K which does not saturate. The common initial slope and the quite sharp decrease of the trailing edge of this peak is a clear indication of a zeroth order desorption. Thus, we can attribute the second peak to desorption from a multilayer which corresponds in

our case, to the crystallites sitting on the one monolayer thick wetting layer of lying p-6P molecules.

As we have seen, the formation of the final surface morphology, dominated by chains [7] can be divided in three steps. First, at low p-6P cover-

age, only 3D crystallites are formed (Fig. 1a). The size evolution of the crystallites as depicted in Fig. 3 is typical for a strain controlled growth mechanism [1, 2]. When more material is deposited the lateral and vertical size of the crystallites saturates quickly and a new entity is formed instead of adding molecules to already existing crystallites. As a result the density of the crystallites per unit area increases almost linearly in the first 30 seconds.

In a second step, crystallites and chains of crystallites coexist (Fig. 1b). This growth morphology starts to evolve as soon as a critical density of crystallites is exceeded locally. For the spontaneous rearrangement of the crystallites we propose the following scenario. The strain that is induced locally by the crystallites into the wetting layer, leads to the formation of a linear defect in the wetting layer (see Fig. 7a) whose orientation is related to the substrate geometry [14]. This defect stimulates the mobile crystallites to touch each other in a specific direction and is so acting as a nucleation center for the chain. The rearrangement process is performed by the crystallites as entities, since we can still recognize the individual crystallites. Once the crystallites are incorporated into the chain they are trapped there, forming a stable nucleus (see threshold length in Fig. 4). It should be noted here that a similar strain induced formation of crystallite chains is observed in SiGe/Si(001) heteroepitaxy. There, misfit dislocations – evolving at the substrate film interface after a critical thickness – guide

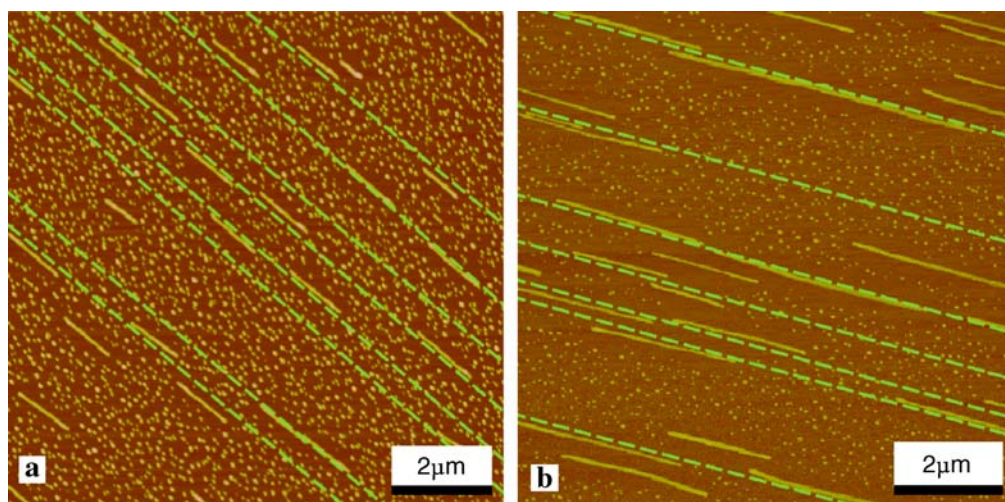


**FIGURE 7** As grown (left) and annealed (right) p-6P on mica(001) film. The dashed green lines indicate the proposed linear defect array. z-scale is 50 nm

3D SiGe crystallites along  $\langle 110 \rangle$  directions [2, 15].

The threshold length of the formed chain is determined by the amount of the excess density. If – in a next step – a new crystallite is formed, the amount of excess density added by a single crystallite is higher as in the preceding step because the area covered by crystallites is now smaller than before (parts of the original area are now covered by the already built chains and their denuded zones). This leads to the formation of a longer chain because more material has to be removed from the area covered with crystallites. This can be done by either extending an existing chain, or by creating a new chain. Such a new chain is either formed using the extended linear defect induced by an already existing chain in the vicinity, or by inducing a new line defect finally resulting in a one-dimensional defect array. The former case is vividly seen in Fig. 7a where frequently two or more chains line up along the same linear defect. When a certain number of chains is formed the density increases less since there is always a chain close to the newly formed crystallite that can be extended.

If the growth is interrupted at this point and the sample is kept at the deposition temperature for a certain time (annealing), a further reduction of the strain can be achieved by incorporation of surrounding crystallites into the already existing chains. Usually, no more new chains are formed during this annealing process. This can be understood, if one takes into account that no more new crystallites will be formed during annealing. As the critical density that is necessary to induce the linear defect can not be exceeded no new nucleation centers are formed. However, if a new chain is formed during the annealing process it has to use one of the

already existing nucleation centers and is therefore always aligned with a previously formed, and therefore, longer chain. The experimental result of such an annealing is displayed in Fig. 7b. Indeed, we observe an increase in the average length of the chains, but no increase in the density of the defect array. Furthermore, this experiment is an additional hint that the crystallites are mobile.

In a third stage, no more crystallites are formed on the wetting layer because the surface is completely covered with chains and their capture zones (Fig. 1c) start to overlap. New material is either included directly at the ends of existing chains or new crystallites are formed on top of them (insert in Fig. 1c).

#### 4 Conclusions

p-6P growth on the highly anisotropic mica(001) surface has been investigated in detail by AFM. Three different growth morphologies depending on the amount of deposited material have been observed. The first growth stage is dominated by the formation of strain controlled randomly arranged 3D crystallites. The second stage is characterized by a coexistence of these mobile crystallites and parallel running chains with defined threshold lengths which are surrounded by depleted zones, due to rearrangement of the crystallites. The driving force for the spontaneous formation of the chains is a critical density of the crystallites that locally induces a linear defect in the monomolecular wetting layer. When this density is reached no more crystallites can be formed without interfering with already existing entities. Further deposition of material leads to the third growth stage, where only p-6P chains are observed. For the future, in situ growth experiments are planned in order to verify that the crystallites con-

taining about 140 000 molecules indeed self-organize as entities into nanofibers as is indicated by the interior chain structure.

**ACKNOWLEDGEMENTS** We thank Stefan Müllegger and Dr. Roland Resel (TU Graz) for fruitful discussions. The research was supported by the Austrian science fund within the project cluster “Highly Ordered Organic Epilayers” (especially, FWF Projects P-15155, P-15625, P-15626, P-15627). Part of this work was performed within the Christian Doppler society’s dedicated laboratory on plastic solar cells funded by the Austrian ministry of economic affairs and Konarka Austria GmbH.

#### REFERENCES

- 1 V.A. Shchukin, D. Bimberg, *Rev. Mod. Phys.* **71**, 1125 (1999)
- 2 C. Teichert, *Phys. Rep.* **365**, 335 (2002)
- 3 S.R. Forrest, *Chem. Rev.* **97**, 1793 (1997)
- 4 P. Fenter, P.E. Burrows, P. Eisenberger, S.R. Forrest, *J. Cryst. Growth* **152**, 65 (1995)
- 5 P. Fenter, F. Schreiber, L. Zhou, P.E. Eisenberger, S.R. Forrest, *Phys. Rev. B* **56**, 3046 (1997)
- 6 A. Andreev, C. Teichert, G. Hlawacek, H. Hoppe, R. Resel, D.M. Smilgies, H. Sitter, N.S. Sariciftci, *Org. Electron.* **5**(1–3), 23 (2004)
- 7 A. Andreev, G. Matt, C.J. Brabec, H. Sitter, D. Badt, H. Seyringer, N.S. Sariciftci, *Adv. Mater.* **12**(9), 629 (2000)
- 8 H. Plank, R. Resel, S. Purger, J. Keckes, A. Thierry, B. Lotz, A. Andreev, N.S. Sariciftci, H. Sitter, *Phys. Rev. B* **64**, 235423 (2001)
- 9 F. Balzer, H.G. Rubahn, *Appl. Phys. Lett.* **79**(23), 3860 (2001)
- 10 H. Plank, R. Resel, A. Andreev, N.S. Sariciftci, H. Sitter, *J. Cryst. Growth* **237–239**, 2076 (2002)
- 11 K.N. Baker, A.V. Fratini, T. Resch, W.W. Adams, E.P. Socciand, B.L. Farmer, *Polymer* **34**(8), 1571 (1993)
- 12 A. Lopez-Otero, *Thin Solid Films* **49**(1), 3 (1978)
- 13 S. Müllegger, O. Stranik, E. Zojer, A. Winkler, *Appl. Surf. Sci.* **221**(1–4), 184 (2004)
- 14 H. Plank, R. Resel, H. Sitter, A. Andreev, N.S. Sariciftci, G. Hlawacek, C. Teichert, A. Thierry, B. Lotz, *Thin Solid Films* **443**(1–2), 108 (2003)
- 15 D.E. Jesson, K.M. Chen, S.J. Pennycook, T. Thundat, R.J. Warmack, *Science* **268** (5214), 1161 (1995)